Dynamic investigation of congestion management methods for dynamic security assessment application

Ines Hauer[1,*], Marc Richter[2], and Chris Oliver Heyde[3]

[1] Institute of Electrical Power Systems, Otto-von-Guericke-University, Magdeburg, Germany
[2] Fraunhofer Institute for Factory Operation and Automation IFF, Magdeburg, Germany
[3] Siemens AG, Germany

***Abstract* – The large share of renewables in the generation mix and concomitant upgrading of the grid into a smart grid is making system operation more complex and highly dynamic. This necessitates swifter responsiveness to changes in system states in order to operate highly loaded grids in which dynamic security limits will likely become increasingly critical. Dynamic security assessment can be applied to detect potential hazards and to assist operators by recommending optimized countermeasures. This paper is focused on the identification of countermeasures against congestion, which can be employed in dynamic security assessments.**

These problems are generally counteracted by preventive redispatch using conventional power plants located far away. Managing the situation with technical efficiency requires factoring in distributed energy resources and loads. Based on a literature review, an extended Newton-Raphson algorithm has been chosen for this purpose. The algorithm has been modified to calculate optimal redispatch, factoring in loads, generators and slack generators. Optimal in this case denotes the most effective technical measures and solutions identified, which will return the system to its normal state with a minimum of adjustments. The suitability of the redispatch method is subsequently tested in a dynamic security assessment system. The results of the dynamic test reveal the utility of the proposed method. The redispatch amount can be reduced by factoring in generator performance after a fault.

* Corresponding author.
E-mail: ines.hauer@live.de

http://dx.doi.org/10.25729/esr.2018.02.0002
Received: April 13, 2018. Revised: May 31, 2018. Accepted: June 13, 2018. Available online: October 15, 2018.

***Index Terms* — dynamic security assessment, system operation, redispatch, congestion**

I. Introduction

The tremendous increase in renewable energy sources (RES) makes it necessary to upgrade the grid into a smart grid in which all system actors are coordinated smartly with communication architecture to observe system security limits. Rapid changes in the power balance caused by the volatility of renewables necessitate a system that responds more rapidly to changes in state. In 2015, the maximum quarter hourly change in wind power injected by Wind Energy Association (WEA) was 1.43 GW in eastern Germany [1]. Closure of conventional power plants is another challenge to system operation. Reducing the rotating mass and system time constants causes system states to change faster. Furthermore, high power flows through the lines and highly volatile generation lead to high utilization of the system where dynamic security limits can become more critical than static security limits. "Security of a power system refers to the degree of risk in its ability to survive imminent disturbances (contingencies) without interruption of customer service." [2]. A distinction is made between static and dynamic security analysis. The first, which is implemented in control centers at present, employs steady-state modeling to analyze whether equipment is overloaded and voltage limits are being observed after a fault. Dynamic security analysis involves different categories of system stability. A power system is considered stable "if it is able to regain a state of operating equilibrium, for a given initial operating condition, after being subjected to a physical disturbance, with most system variables bounded so that practically the entire system remains intact" [2]. Power system stability is broken down into rotor angle stability, voltage stability, and frequency stability, specifying a variety of phenomena contingent on different time scales. [3] [4]. A dynamic security assessment (DSA) tool can assists system

operators in this new operating environment [5], [6] by analyzing these stability categories. Taking the system's current operating point as the point of departure, potential threats to the system can be detected by means of an index and a contingency analysis. This data can be used to calculate the most effective countermeasures adapted to the system's operating point, the fault and the resulting stability problem [7] [8].

Methods for detecting voltage stability and eliminating voltage instability [9], [10] and automatic protection schemes [11] have been widely discussed. This paper focuses on congestion management. Given the large share of RES installed in Germany, congestion management is routine for German transmission system operators and their systems are operating close to their static security limits. Supply failures or rapid changes in weather can cause further congestion but conventional redispatch capacities are depleted. Every flexibility option has to be included to ascertain the most effective countermeasures in order to keep the system within its stability limits. This requires the capability to coordinate all actors in the system intelligently by means of a communication infrastructure. In Germany in particular, the incoming supply of renewables can be adjusted as part of system security management. Moreover, specifications are being developed at this time for controllable loads (active power and reactive power adjustment), which are operated by demand-side management systems (regulations for switchable loads).

Since congestion problems are normally not as time sensitive as short circuits, they are modeled with steady-state methods. Redispatch has to be employed technically efficiently in heavily utilized systems with a large share of volatile generating and falling system time constants. This makes dynamic security analysis factoring in generator performance increasingly more interesting for the resolution of congestion problems.

In this paper, we focus on countermeasures against congestion with the intention to implement them in an existing DSA tool. Steady-state modeling methods for ascertaining optimal redispatch are analyzed in order to keep the algorithms simple and expedite calculations. Every system component, especially loads, generators and the slack generator, have to be considered to identify the most technically efficient redispatch. Optimal in this case denotes the most effective technical measures and solutions identified, which will return the system to its normal state with a minimum of adjustments. Since stabilizing a system with optimal adjustment minimizes the probability of the other critical system states arising from the countermeasure applied, cost-effective redispatch algorithms are not applied. Finally, the algorithm was implemented in an existing DSA tool to gauge the extent to which it can be applied in dynamic security assessment programs.

II. Literature review

The literature presents different methods for determining effective generator combinations and adjusting their power to prevent congestion. A good overview is provided in [12].

One frequently discussed and applied method is based on the Power Transfer Distribution Factor (PTDF) [13] [14]. The PTDF depicts the effects of single generators or network nodes on single lines and determines the available transmission capacity (ATC) of lines [15], [16]. The PTDF's good approximations of the conventional Newton-Raphson (NR) method for calculating the ATCs are demonstrated in [17]. Most algorithms with technically effective solutions are based on the standard NR algorithm for load flow analysis or fast decoupled load flow analysis, which is a simplification of the NR [18] used to analyze load flows in high voltage grids. Numerous algorithms treat redispatch as a market measure and employ optimization algorithms to select generators based on their cost-effectiveness [19], [20], [21]. A day-ahead congestion forecast is used in [22] and [23] to incentivize to shift the load by using price signals such as demand-side response. The demand management or load scheduling can be attractive because of its current potential, particularly in the industry [24]. Cost-based redispatch using generators and loads is presented in [25] and [26]. Suitable components are selected by a sensitivity analysis, which is based on a decoupled power flow calculation and the costs of active power adjustment. Here, generators are preferable to loads. An electrical distance concept for generators [27] or intelligent technique of particle swarm optimization [28] is also used to optimize rescheduling measures factoring in market issues. The authors of [29] test the effect of three parameters on the redispatch amounts and costs: loop flows through the electricity system, an increase in renewable generation, and a remedial and preventive N-1 security criterion in a model of the Belgian power system. Additionally, [30] focuses on redispatch costs and the authors have improved LMP to incorporate the energy price, congestion revenue, financial losses and the transmission usage fee by utilizing optimal power flows based on shift factors.

The need to factor distributed generation into rescheduling measures has grown in recent years. Since congestion also occurs in distribution systems [31], the placement of distributed generation in a power system [32], its use for rescheduling, and the balance between costs social factors have to been taken into account [33].

Costs are of secondary importance when the risk of system instability is high. Then, technically efficient redispatch utilizing every available component is required to restore the system. An extension of the Newton-Raphson algorithm that ascertains technically efficient generator **r**edispatch (ENRA-R) is presented in [34]. A line sensitivity matrix is used to identify the generators that

have maximum influence on the line. The power that has to be adjusted at the generators is calculated with the aid of an extended Jacobian matrix. The algorithm has been tested and verified in a European system model with 1254 nodes and 379 generators. This static method was selected and expanded for the tests in this paper since several line limits can be considered simultaneously and loads can be shed with this method, which can be applied to every voltage level. The ENRA-R method had to be extended for this study since the method in [34] did deliver the correct sensitivities when selecting the most efficient network node. The new extended method is verified by comparing the results from it with results from the standard PTDF algorithm.

This paper is organized as follows. After briefly defining redispatch, the mathematical principles of ENRA-R and its extension are presented. This method was implemented and tested in a 30-node IEEE test system to demonstrate the need for the aforementioned extension. The results were compared with the results of the PTDF method, which was also implemented. Finally, the ENRA-R was implemented in a dynamic security assessment system to calculate optimal redispatch for a sudden congestion problem. The applicability of the proposed method in DSA is demonstrated.

III. The Methodology

Network operators normally detect impending static congestion problems well before they occur and respond with the market-based countermeasure of redispatch, i.e. by adjusting production in power plants to protect lines from overloading. The principle is presented in Fig. 1. The following scenario is considered: following a single line outage in a double line, the second line is overloaded. Eliminating congestion requires reducing generation before the congestion (Fig. 1, area 1) and increasing generation after the congestion by the same amount (Fig. 1, area 2).

In a smart grid, not only conventional generation but also all system components have to be considered to solve the problem efficiently with minimum adjustment. The switch off and on of loads as well as renewable generation control are therefore taken into account in this study to identify the most effective redispatch measures.

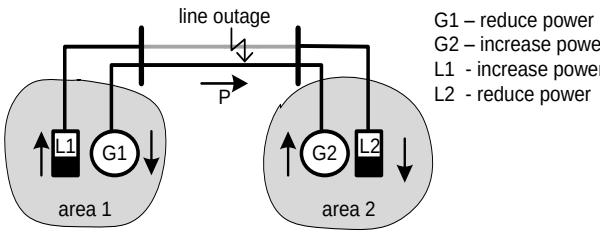

Figure 1. Principle of redispatch.

A. Determining the Optimal Redispatch Combination

1) The ENRA-R Method

The ENRA-R method introduced here is largely based on a publication by Glavich et al. [34]. The authors use the algorithm to determine the optimal adjustment of generation to solve a congestion problem. It is modified to become the ENRA-RM method, which incorporates the slack generator disregarded in [34] and loads for redispatch.

ENRA-R is based on the standard NR method [18], typically the method of choice for solving a system of nonlinear equations. Under steady-state conditions, the power flow equations are defined with Kirchoff's law as

$$\boldsymbol{f}(\boldsymbol{x}) = \begin{pmatrix} \Delta \boldsymbol{P}(\boldsymbol{x}) \\ \Delta \boldsymbol{Q}(\boldsymbol{x}) \end{pmatrix} = 0 \tag{1}$$

where x is the vector of the state variables (phase angles δ and bus voltage magnitude U). Taking an initial operating point (x_0) as the starting point, the solution is obtained iteratively.

$$\begin{bmatrix} \Delta \boldsymbol{P} \\ \Delta \boldsymbol{Q} \end{bmatrix} = \begin{bmatrix} \boldsymbol{H} & \boldsymbol{N} \\ \boldsymbol{M} & \boldsymbol{L} \end{bmatrix} \begin{bmatrix} \Delta \boldsymbol{U} \\ \Delta \delta \end{bmatrix}; \begin{bmatrix} \Delta \boldsymbol{P} \\ \Delta \boldsymbol{Q} \end{bmatrix} = \boldsymbol{J} \begin{bmatrix} \Delta \boldsymbol{U} \\ \Delta \delta \end{bmatrix} \tag{2}$$

with $$\boldsymbol{H} = \frac{\partial \boldsymbol{P}}{\partial \boldsymbol{\delta}}; \boldsymbol{N} = \frac{\partial \boldsymbol{P}}{\partial \boldsymbol{U}}; \boldsymbol{M} = \frac{\partial \boldsymbol{Q}}{\partial \boldsymbol{\delta}}; \boldsymbol{L} = \frac{\partial \boldsymbol{Q}}{\partial \boldsymbol{U}}$$

The elements of the Jacobian matrix $\boldsymbol{J}$ are the partial derivatives with respect to voltage U and voltage angle δ according to (1) [18].

The Jacobian matrix is used to identify system components suitable for efficient redispatch, in this case, generators and loads. The active power flow through the line is reduced to rectify line congestion, while the reactive power flow is disregarded [35]. Apparent power or current can also be specified as a limit, however.

The line flow can be defined as a ''sending terminal'' or ''receiving terminal'' flow (sending and receiving terminals being the two ends of a transmission line) to ascertain the sensitivities of flows through lines of interest. Sending terminal flows are worked with here. The terminal admittance matrix $\boldsymbol{Y}_T$ is defined to simplify the power flow equations that determine "sending terminal flows". $\boldsymbol{Y}_T$ is the primary admittance matrix in which the diagonal elements are a small admittance matrix (2-port representation of branch and transformer) [36]. Each matrix's rows therefore have only two nonzero elements, one at the sending and the other at the receiving end of the branches. Multiplying $\boldsymbol{Y}_T$ by the vector of complex terminal voltages $\underline{\boldsymbol{u}}_T$ yields the vector of terminal current $\underline{\boldsymbol{i}}_T$ for all branches. Sign identification identifies the terminal nodes with positive currents $\underline{\boldsymbol{i}}_k$ for each branch k. The

vector of complex sending terminal voltages is denoted by $\underline{\boldsymbol{u}}_{\mathrm{k}}$.

$$\underline{\boldsymbol{s}}_{\mathrm{k}} = 3\ \mathrm{diag}(\underline{\boldsymbol{u}}_{\mathrm{k}})\boldsymbol{Y}_{\mathrm{T}}^{*}\underline{\boldsymbol{u}}_{\mathrm{T}}^{*} \tag{3}$$

When U_{k} denotes the voltage at the sending terminal of branch k and $\delta_{\mathrm{ki}} = \delta_{\mathrm{k}} - \delta_{\mathrm{i}}$, then the apparent power flow s and the active power flow p on branch k can be calculated from (4) and (5) where G_{ki} and B_{ki} are the real and imaginary parts of admittance between the buses k and i.

$$\underline{\boldsymbol{s}}_{\mathrm{k}} = 3 \sum_{\underline{Y}_{\mathrm{T}}^{\mathrm{ki}} \neq 0} U_{\mathrm{k}} U_{\mathrm{i}} \delta_{\mathrm{ki}} (G_{\mathrm{ki}} - \mathrm{j}\, B_{\mathrm{ki}}) \tag{4}$$

$$\boldsymbol{p}_{\mathrm{k}} = 3 \sum_{\underline{Y}_{\mathrm{T}}^{\mathrm{ki}} \neq 0} (U_{\mathrm{k}} U_{\mathrm{i}} G_{\mathrm{ki}} \sin\delta_{\mathrm{ki}} + U_{\mathrm{k}} U_{\mathrm{i}} B_{\mathrm{ki}} \cos\delta_{\mathrm{ki}}) \tag{5}$$

The flow Jacobian $\boldsymbol{J_f}$ that specifies the effect of voltage and angle changes on the active power flow change through the line is determined to ascertain the sensitivity of the active power flow, which is a function of the change of the active power at the node.

$$\Delta \boldsymbol{p}_{\mathbf{f}} = \boldsymbol{J}_{\mathrm{f}} \cdot \begin{bmatrix} \Delta \boldsymbol{U} \\ \Delta \boldsymbol{\delta} \end{bmatrix} \quad \text{with} \quad \boldsymbol{J}_{\mathrm{f}} = [\, \boldsymbol{H}_{\mathbf{f}} \ \ \boldsymbol{N}_{\mathbf{f}} \,] \tag{6}$$

where

$$H_{\mathrm{f}}^{\mathrm{ki}} = \begin{cases} 0 & \text{if } Y_{\mathrm{T}}^{\mathrm{ki}} = 0 \\ -3U_{\mathrm{k}}U_{\mathrm{i}}G_{\mathrm{ki}}\sin\delta_{\mathrm{ki}} + 3U_{\mathrm{k}}U_{\mathrm{i}}\cos\delta_{\mathrm{ki}} & \text{if } \mathrm{k} \neq \mathrm{i} \\ 6U_{\mathrm{k}}G_{\mathrm{ki}} & \text{if } \mathrm{k} = \mathrm{i} \end{cases} \tag{7}$$

$$N_{\mathrm{f}}^{\mathrm{ki}} = \begin{cases} 0 & \text{if } Y_{\mathrm{T}}^{\mathrm{ki}} = 0 \\ 3U_{\mathrm{k}}G_{\mathrm{ki}}\cos\delta_{\mathrm{ki}} + 3U_{\mathrm{k}}\sin\delta_{\mathrm{ki}} & \text{if } \mathrm{k} \neq \mathrm{i} \\ 6U_{\mathrm{k}}G_{\mathrm{ki}} & \text{if } \mathrm{k} = \mathrm{i} \end{cases} \tag{8}$$

Equation (2) is transformed and inserted into (6) to ascertain the effect of a change in the active power injection on the active power flow through the line. The sensitivity matrix $\boldsymbol{S}$ is determined from (9) and (10).

$$\Delta \boldsymbol{P}_{\mathrm{f}} = \boldsymbol{J}_{\mathrm{f}} \cdot \boldsymbol{J}^{-1} \begin{bmatrix} \Delta \boldsymbol{P} \\ \Delta \boldsymbol{Q} \end{bmatrix} \tag{9}$$

$$\boldsymbol{S} = \boldsymbol{J}_{\mathrm{f}} \cdot \boldsymbol{J}^{-1} \tag{10}$$

$\boldsymbol{S}$ describes the influence of an active power change $\Delta\boldsymbol{P}$ or reactive power change $\Delta\boldsymbol{Q}$ at the system nodes on the active power flows $\Delta\boldsymbol{P}_{\mathrm{f}}$ of all lines. According to [34], active power can be adjusted at every node except the slack node, whereas reactive power can only be adjusted at PQ or load nodes.

2) The ENRA-RM Method

The reference generator for redispatch cannot be selected in the algorithm presented in [34] because of the singularity of the Jacobian. The active and reactive power equations of the reference node and the reactive power equations of the generator nodes at which the voltage is kept constant are removed from the Jacobian matrix in order to render it invertible. This can lead to falsification of the sensitivity matrix, which is determined from the inverted Jacobian using (10). For instance, if the sensitivity of the reference generator for the analyzed line is very large, this omission falsifies the sensitivities of other generators.

The method of power flow decomposition [37] [36] can be employed to invert the full Jacobian. The power flow equation based on (11) and (12) with the nodal admittance matrix $\boldsymbol{Y}_{\mathrm{KK}}$ is linearized in the current operating point with the assumption that voltages at nodes K are constant.

$$\underline{\boldsymbol{s}}_{\mathrm{K}} = 3\ \mathrm{diag}(\underline{\boldsymbol{u}}_{\mathrm{K}})\boldsymbol{Y}_{\mathrm{KK}}^{*}\underline{\boldsymbol{u}}_{\mathrm{K}}^{*} = 3\ \underline{\boldsymbol{U}}_{\mathrm{K}}\boldsymbol{Y}_{\mathrm{KK}}^{*}\underline{\boldsymbol{u}}_{\mathrm{K}}^{*} \tag{11}$$

$$(\underline{\boldsymbol{U}}_{\mathrm{K}}^{-1}\underline{\boldsymbol{s}}_{\mathrm{K}}/3)^{*} = \boldsymbol{Y}_{\mathrm{KK}}\underline{\boldsymbol{u}}_{\mathrm{K}} = \underline{\boldsymbol{i}}_{\mathrm{K}} \tag{12}$$

The next step will be to divide nodal currents $\underline{\boldsymbol{i}}_{\mathrm{K}}$ into generation currents (index G) and load currents (index L).

$$\boldsymbol{Y}_{\mathrm{KK}}\underline{\boldsymbol{u}}_{\mathrm{K}} = \underline{\boldsymbol{i}}_{\mathrm{K,L}} + \underline{\boldsymbol{i}}_{\mathrm{K,G}} = (\underline{\boldsymbol{U}}_{\mathrm{K}}^{-1}\underline{\boldsymbol{s}}_{\mathrm{K,L}}/3)^{*} + (\underline{\boldsymbol{U}}_{\mathrm{K}}^{-1}\underline{\boldsymbol{s}}_{\mathrm{K,G}}/3)^{*} \tag{13}$$

The load currents are converted into nodal admittances $\boldsymbol{Y}_{\mathrm{K,L.}}$ based on (14). Conversion can only be done for the particular operating point.

$$\underline{\boldsymbol{i}}_{\mathrm{K,L}} = \boldsymbol{Y}_{\mathrm{K,L}}\underline{\boldsymbol{u}}_{\mathrm{K}} = (\underline{\boldsymbol{U}}_{\mathrm{K}}^{-1}\underline{\boldsymbol{s}}_{\mathrm{K,L}}/3)^{*} \tag{14}$$

Only loads not intended for redispatch are formulated as node matrices $\boldsymbol{Y}_{\mathrm{K,L1}}$ to determine the sensitivity matrix $\boldsymbol{S}$. Converting one equivalent node admittance suffices in this case.

$$\boldsymbol{Y}_{\mathrm{KK}}\underline{\boldsymbol{u}}_{\mathrm{K}} = \boldsymbol{Y}_{\mathrm{K,L1}}\underline{\boldsymbol{u}}_{\mathrm{K}} + (\underline{\boldsymbol{U}}_{\mathrm{K}}^{-1}\underline{\boldsymbol{s}}_{\mathrm{K,L2}}/3)^{*} + (\underline{\boldsymbol{U}}_{\mathrm{K}}^{-1}\underline{\boldsymbol{s}}_{\mathrm{K,G}}/3)^{*} \tag{15}$$

Then, the equivalent admittances $\boldsymbol{Y}_{\mathrm{K;L1}}$ are integrated in the admittance matrix $\boldsymbol{Y}_{\mathrm{KK}}$ resulting in $\boldsymbol{Y}_{\mathrm{KK}}$', a different form of $\boldsymbol{Y}_{\mathrm{KK.}}$

$$(\boldsymbol{Y}_{\mathrm{KK}} - \boldsymbol{Y}_{\mathrm{K,L1}})\underline{\boldsymbol{u}}_{\mathbf{K}} = (\underline{\boldsymbol{U}}_{\mathrm{K}}^{-1}\underline{\boldsymbol{s}}_{\mathrm{K,L2}}/3)^{*} + (\underline{\boldsymbol{U}}_{\mathrm{K}}^{-1}\underline{\boldsymbol{s}}_{\mathrm{K,G}}/3)^{*} \tag{16}$$

$$\boldsymbol{Y}'_{\mathrm{KK}}\underline{\boldsymbol{u}}_{\mathbf{K}} = \underline{\boldsymbol{i}}_{\mathrm{K,L2}} + \underline{\boldsymbol{i}}_{\mathrm{K,G}} = \boldsymbol{i}'_{\mathrm{K}} \tag{17}$$

Employing $\boldsymbol{Y}_{\mathrm{KK}}$' instead of $\boldsymbol{Y}_{\mathrm{KK}}$ in the load flow calculation yields the same results, the important difference being that the Jacobian matrix determined from $\boldsymbol{Y}_{\mathrm{KK}}$' is regular and invertible. For this reason, the slack node row and slack node column in the Jacobian matrix do not have to be removed and can be factored into redispatch.

3) Determining Suitable Redispatch Combinations

The influence of all generators, including the reference generator, and the loads on the lines are determined by using the full Jacobian matrix to determine the sensitivity matrix based on (10). This method is only used to determine sensitivities. The standard Jacobian matrix is incorporated in all other algorithms.

When the intention is to perform redispatch by adjusting generation, only the sensitivities S_G of the generator nodes are considered. By contrast, all PQ elements S_{PQ} must be used when only load adjustment is being considered. This yields three possible component combinations that reduce power before the line congestion (area 1 in Fig. 1) and increase power by roughly the same amount after the congestion (in area 2 in Fig. 1).

Redispatch is presently only performed by generators so that supply is not disrupted. The flexible loads available in a future smart grid will be usable for congestion management to stabilize the system as quickly as possible.

Three different load generation combinations were analyzed (see Table 1), whereas the generator and load combination represents disconnection of load and generation (e.g. RES).

The components with the maximum impact on the affected line are selected to calculate efficient redispatch. To this end, the corresponding line of the sensitivity matrix is determined. Subsequently, the nodes of interest (e.g. the PQ nodes, generator nodes or all nodes) are filtered and sorted according to size. The generator with the highest line sensitivity and the generator with the lowest line sensitivity are selected to reduce or increase their active power output ΔP_r.

B. Determining the Required Power Adjustment

Once the appropriate components have been selected, the required power adjustment ΔP_r has to be determined. The extension of the NR algorithm is used. First, the Jacobian $\boldsymbol{J}$ is determined by the load flow calculation with its elements H, N, M and L. Second, the matrix is extended by one row and one column, which define an additional condition [34].

$$\begin{bmatrix} \Delta P \\ \Delta Q \\ \Delta P_L \end{bmatrix} = \left[\begin{array}{cc:c} H & N & k1 \\ M & L & \\ \hdashline FF1 & & 0 \end{array}\right] \begin{bmatrix} \Delta\delta \\ \Delta U \\ \Delta P_r \end{bmatrix} \tag{18}$$

$$\Delta P_L = P_{line} - P_{line\ limit} \tag{19}$$

In (19), ΔP_L represents the change in active power flow needed through the line so that the line is not overloaded. The limit of power flow through the lines is given by the maximal current or is defined by the system operator, who has to take into account n-1 criteria. The vector *k1* represents the nodes selected from S at which active power should be adjusted ΔP_r. The node at which the active power should be increased by ΔP_r is specified in vector k1 by +1 and the node at which the active power should be reduced by ΔP_r is specified by -1. When loads are used, the reactive power also has to be adjusted. To do this, the relationship between active and reactive power is assumed to remain constant.

The term $FF1$ represents the active power sensitivities at the sending node of the affected line and is results from the J_{PF} elements of the line based on (9). The solution of ENRA-R includes the power to be adjusted ΔP_r in the components selected.

Table 1. Redispatch combinations.

Combination	Sensitivities	Component in area 1	Component in area 2
Generator and generator	Generator nodes $S \rightarrow S_G$	Gen. at node max(S_G): $\Delta P_r\downarrow$	Gen. at node min(S_G): $\Delta P_r\uparrow$
Generator and load	All nodes $S \rightarrow S_G$ & S_{PQ}	Gen. at node max(S_G): $\Delta P_r\downarrow$	Load at node max(S_{PQ}):$\Delta P_r\downarrow$
Load and load	Only PQ nodes $S \rightarrow S_{PQ}$	Load at node min(S_{PQ}):$\Delta P_r\uparrow$	Load at node max(S_{PQ}):$\Delta P_r\downarrow$

Table 2. Redispatch test scenarios in the 30-node test system.

Lines	Power flow in initial state in MW	Power flow in target state in MW
Line 6	19.86	15
Line 3	13.63	10 / 12
Line 32	17.67	12

IV. Results of Implementation of ENRA-RM

A. Steady-State Test Power System

The algorithms were tested in a 30-node test system consisting of a 135 kV high voltage power system consisting of six generators, twenty loads and forty-one lines (see Fig. 2) [38], [39]. The loading of the lines selected in the initial state and the target state with a lower power flow is demonstrated in Table 2. The power limitations specified are assumed values that demonstrate the functionality of redispatch using the scenarios presented.

1) Results of the Steady-State Test

First, the redispatch algorithms are tested statically. The reduction of the power flow on the lines specified in Table II is tested with different scenarios, namely:

a. technically effective redispatch by adjusting active power to generators,

b. technically effective redispatch by adjusting load and active power to generators, and

c. technically effective redispatch by adjusting load.

a) Technically Effective Redispatch by Adjusting Active Power to Generators

The difference between the sensitivity matrix calculation based on the reduced Jacobian in [34] (principle 1) and the full Jacobian (principle 2) is presented as introduction.

The generator sensitivities of line 32 are presented in Table 3, the power flow in this line limited to 12 MW. The algorithm selects the generator with the highest sensitivity (G23) to reduce power and the generator with the lowest sensitivity (G27) to increase power. Sensitivities indicated by a positive sign are usually suited to reduce power to

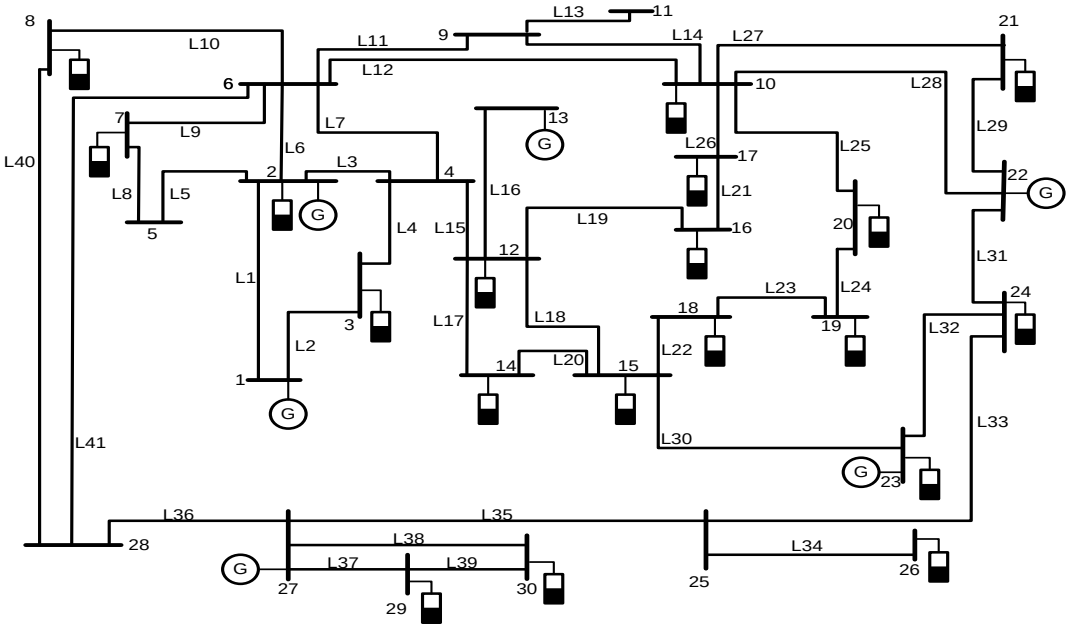

Figure 2. Test power system based on [38].

lower the power flow over the line, while sensitivities indicated by a negative sign or a small sensitivity are usually suited to increase power. The generators that increase power have little impact on the line power flow, their power input have to be adapted to balance the system.

When a generator is operated close to the limit or is unavailable for redispatch, the generator with the next lower or next higher sensitivity is selected. Reasons for generator unavailability vary. The efficiency of power plants at different operating points is not an exclusion criterion in this case since every generator has to contribute to system stability. Exclusion criteria are the necessity of the allowance of control reserve or maintenance actions.

Table 3 reveals that G23 has the largest sensitivity and G27 has the lowest sensitivity in both principles. If G27 is unavailable for redispatch, then G13 and G2 are chosen to increase power in principle 1. Following principle 2, the order is G27, G22 and, finally, G1.

Some results for principle 1 are compiled in Table 4. For test purposes, the upper limit of the generators G27 or G13 varies so that they are not always available for redispatch. Since the power output of G27 cannot be increased in case 2, G13 is chosen. Since G13 is at its upper limit in case 3, too, G2 has to be selected instead of G27 or G13. The same tests are repeated for principle 2. The results are compiled in Table 5, G22 being unavailable in case 3 and G1 being unavailable in case 4.

As evidenced by the results in Table 4, the use of G2 is considerably more efficient. Even though its sensitivity is lower than that of G13, the use of G2 requires less total power adjustment. The analysis of sensitivities in principle 2 reveals that G13 has a positive sign and is, thus, better suited for decreasing power, while G2 is the better option for increasing power.

Table 3. Generator sensitivities of line 32, principle 1 (P1): without slack node in G1, principle 2 (P2): with slack node in G1

	G1	G2	G13	G22	G23	G27
P1	-	-0.0008	-0.0329	0.372	0.4253	-0.0745
P2	0.0008	0.0016	0.1095	-0.0863	0.4304	-0.1039

Table 4. Influence of generators on line 32, principle 1

	Available Generators	Generators	ΔP_r [MW]
Case 1	G2, G23, G22, G13, G27	G23↓, G27↑	10.34
Case 2	G2, G23, G22, G13	G23↓, G13↑	17.93
Case 3	G2, G23, G22	G23↓, G2↑	13.30

Table 5. Influence of generators on line 32, principle 2

	Available Generators	Generators	ΔP_r [MW]
Case 1	G13, G2, G23, G1, G22, G27	G23↓, G27↑	10.34
Case 2	G13, G2, G23, G1, G22	G23↓, G22↑	11.00
Case 3	G2, G23, G13, G1	G23↓, G1↑	12.93
Case 4	G2, G23, G13	G23↓, G2↑	13.27

Determination of the sensitivity matrix, including the reference generator, demonstrably results in significantly more efficiency (less power being rescheduled). Consequently, this method is employed in further research.

b) Technically Effective Redispatch by Adjustment Active Power to Loads

Demand-side management systems operate controllable

loads in smart grids, thus adjusting them in critical grid situations for redispatch. A method for managing congestion by means of flexible loads is presented in [40]. Flexible electricity prices in response to line congestion can produce incentives to adjust loads to counteract congestion. In this case, loads can be adjusted in both positive and negative directions. This is easily implemented in energy storage systems that can be used as a controllable source or as a controllable sink in a smart grid. Wind power [41] and PV [42] can be combined with the storage system to coordinate balancing zones better [43] and, in this case, integrate local generation and loads in rescheduling more efficiently. Furthermore, the batteries in electric cars could be used [44] for this task, especially if the core standards for communication have been defined [45].

This makes a combination of load and generator adjustment particularly interesting. Congestion is counteracted by reducing generation in one area and a load in the other area. This constitutes a simple and practicable redispatch combination. Disconnecting loads is much easier than connecting a load. The supply from renewable energy generators, e.g. wind turbines and PV, can also be reduced or switched off in addition to power plants when reducing generation. Switching on renewables is difficult to manage, though, because of their dependence on the weather. Assuming that loads in the system are controllable, we can consider three different combinations. Redispatch incorporating controllable loads is applied in the algorithm ENRA-RM for line 32, in which the power flow should be limited to 12 MW. The results are presented in Table 6.

Adjusting loads for redispatch clearly requires less overall power adjustment. The optimal combination is contingent on the network structure and the controllable components located near the congested line. Table 7 presents an overview of the results of reducing the power flow in different lines of the 30-node test system. ΔP_r is calculated for the three component combinations to reduce the power flow through lines 1-12 by around ΔP_L.

Since more loads are distributed throughout the power system than generators, load combinations significantly lessen the adjustment of power in most cases.

A load combination or load-generator combination has to be applied whenever generator combinations cannot be employed to reduce line power flow. For instance, the active power flow through line 8 cannot be reduced to 6 MW with the existing generators. This can only be done by adjusting another 7.1 MW by selecting the load combination and adjusting an additional 1.1 MW by selecting a load-generator combination. Rapidly solving optimal rescheduling reduces the probability of further incidents caused by congestion. In terms of transient stability, an increase of the generators' active power is always accompanied by an increase in their rotor displacement angle. Since this brings the generators closer to the stability limit and synchronism can be lost earlier whenever failure or further congestion occur, adjustments have to be minimized and made using the most efficient combinations. Redispatch is normally considered as a preventive measure and thus often not time-sensitive. Notified of future congestion problems by forecasts, operators apply redispatch before congestion occurs. Given the large quantity of distributed energy sources installed, conventional and especially German power plants usually redispatch in high-wind situations. Conventional redispatch capacities are exhausted if a failure occurs, which results in another congestion problem. In such a case, other smart grid components, e.g. energy storage systems, controllable loads and distributed energy sources, are an efficient alternative to power plants for remedial redispatch. As the ever more distributed renewable energy sources are integrated, the load generator combination is the best option because power must be reduced or shut off on both sides of the bottleneck. This is usually easier than connecting a load. Loads and renewable energy sources are adjusted quickly by converter systems, which have a time advantage over conventional generators.

Table 6. Influence of component combinations on line 32.

Most efficient redispatch combination	Selected elements	ΔP_r [MW]
2 generators	G23↓, G27↑	10.4
2 loads	load 24↓, load23↑	8.4
Load and generation	G23↓, load 24↓	8.4

Table 7. Comparison of ΔP_R based on the component combinations for lines 1-12

Line	ΔP_L in MW	2 generators ΔP_r in MW	2 loads ΔP_r in MW	Load and generator ΔP_r in MW
1	3	**3.5**	9.5	**3.5**
2	3	8	12.6	**7**
3	3.6	10.6	**10**	10.6
4	4	11	**4.5**	10.9
5	2	11.9	**5.8**	**5.8**
6	2	5.3	**5.1**	**5.1**
7	2	4.6	**2.4**	7.6
8	2	12	**5.9**	**5.9**
9	2	12.4	**2.4**	**2.4**
10	2	14.1	**2.3**	**2.3**
11	2	5.2	**4.8**	7.6
12	1	**4.4**	4.7	6.7
8	**6**	**28 (maximum)**	**1.1**	**7.1**

The comparison with a method based on PTDF yields good agreement, the proposed algorithm can be applied.

B. Dynamic Testing of ENRA-RM with SIGUARD®DSA

Transmission systems are continuously analyzed with steady-state algorithms. They display only the outcome of an event or fault, though. Dynamic analyses are used to analyze system performance during the intervening period, i.e. from the beginning of an event or fault until the situation has stabilized. A dynamic security assessment tool addresses this issue. The redispatch measures presented above were calculated with steady-state algorithms. A dynamic test system including the dynamic security assessment (DSA) system simulator SIGUARD®DSA [46] has been selected to verify their applicability to this problem. SIGUARD®DSA employs the power system simulator PSS®Sincal in which the detailed power system and generator models are stored to analyze the system electro-mechanical performance. The DSA addresses voltage stability, transient stability, small-signal stability and protection. In this study, a redispatch measure is tested, which factors in generator performance.

SIGUARD®DSA determines the potential risk of different contingencies [47], [48] for an electrical power system based on a system's current state. To this end, different security indices are implemented, which indicate whether static and dynamic limits are observed or exceeded in a system and check the range to the limits. A distinction is made between global indices, which represent an entire system (e.g. small signal stability, frequency stability), and local indices, which characterize the status of individual system components (e.g. node voltages, angle stability of generators, active power flows through lines and transformers). Each index is a normalized value between 0 and 1, with 0 representing no risk (green), 0.75 denoting a critical state (red) and 1 standing for a blackout (black). A three stage Fuzzy Inference System that allows modeling of a "multivariable-reasoning system" is employed to combine the indices of the individual components into a fuzzy dynamic security index, the system index [49]. By fuzzification and defuzzification of the indices equally distributed along the interval 0 to 1, a multi-stage Fuzzy Inference System sufficiently composes an over-all dynamic performance index. In addition, an adaptive system is designed which readjusts its structure according to the number of active indices [50]. The outcome of the simulation [6] is the DSA tool's determination of an index for every contingency, which characterizes the system's state after the contingency [47]. Other methods of aggregating indices and determining system security are discussed in the literature [51]. In [52] a method is proposed to determine the maximum loading point to detect the probability for long-term voltage instability. The results are used to train a database for an artificial intelligence (AI) classifier based on the Support Vector Machines (SVM) or machine learning-based models. In online application, the SVM classifier support detecting the probability that generators operating at a high reactive power output that can announce a voltage collapse. Other DSA tools use recognition methods, such as support vector machine, artificial neural network and decision tree to reduce time-consuming simulations. These methods save results of offline time-domain simulations in a database and then train a model with decision rules. Online measurements are combined with the model and used to determine the security states of current [53]. In [54] a method is proposed that uses ensemble decision trees and is capable of predicting the security states with high accuracy and indice the confidence of the security states 1 minute ahead of real time.

The system index and the line power flow index (LPFI) are analyzed to verify the proposed method. The LPFI analyzes the power flow through each line during a dynamic simulation of 20 seconds. The limits can be parameterized individually, since the operator may have to take into account the n-1 criteria. In this test, the index becomes 1 when the power flow S reaches 130% of the rated power. The index becomes 0 when the power flow is below 70%. There is a linear relation between both extrema and the index.

The DSA test system represents a transmission system with voltage levels of 230 kV and 500 kV in which seven generators and thirteen loads or compensators are connected to twenty-five nodes. A schematic of the analyzed system is presented in Fig. 3. The system, generator and controller models were developed by Siemens AG.

1) Test Scenarios Description

Different scenarios representing different system loads and different load distributions were developed for this test system. Different contingencies, particularly short circuits at different nodes and different line outages, were implemented and tested for each scenario. Congestion primarily occurs in highly utilized systems with unbalanced load distribution. Moreover, a line outage was identified as the main cause of congestion. The effectiveness of the proposed method was verified in five scenarios, one of which is presented in detail here.

The following procedure is employed to test the redispatch measures:

1. Introduce a fault (contingency) in SIGUARD®DSA, thus causing line congestion.
2. Export steady-state operating point data after the contingency.
3. Use the ENRA-RM method to identify redispatch measures.
4. Implement the measures in the DSA test system.

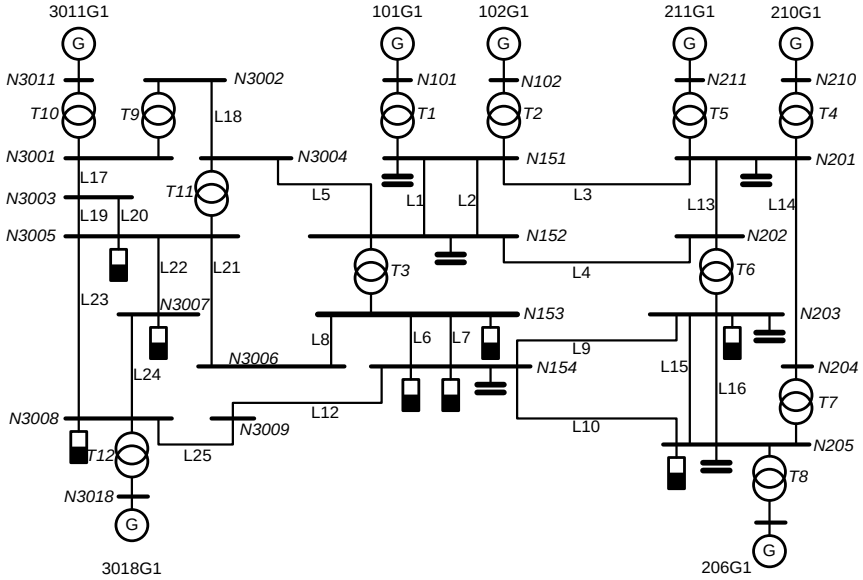

Figure 3. Dynamic test system: DSA system.

2) Test Results

One contingency entailed switching off line 14, thus causing congestion in line 13 and a static frequency deviation of 136 mHz.

The frequency and generator performance are presented in Fig. 4. In the normal state, the frequency is controlled by primary and secondary controls. In this case, generator G211 performed secondary control by reducing its power by about 115 MW. The system reaches a new steady-state operating point after 80 seconds with the active power flow on line 13 reaching 1164.8 MW (see Fig. 4,5, section 2).

The new state variables of voltage magnitude and phase angle and the new power system topology are exported and used as input data for the proposed ENRA-RM method to determine the redispatch measure for that steady-state operating point. In this case, the most efficient component combination and the power to be adjusted is calculated by an ENRA-RM algorithm to reduce the active power flow through line 13 from 1164.8 MW to 1000 MW using (18)

1. Generator combination:
G211↓, G206↑, ΔP_r = 275.6 MW
2. Load-generator combination:
G211↓ L203↓, ΔP_r = 268.4 MW
3. Load combination: not applicable since there are no loads on the 500 kV level

The results of the dynamic calculations for case 1 are presented in Fig. 4 that shows the changes in the active power injection of the generators G211, G206 and 101G1. The effect of this adjustment on the line power flow after 80 seconds and the line index are presented in Figure 5.

The failure (outage of line 14) initiated after 200 milliseconds of simulation time causes the line to overload, indicated by an LPFI above 0.9 and a frequency deviation of 136 mHz (Fig. 4, section 1). This deviation is compensated by primary and secondary control of generators within the next 80 seconds. Subsequently, the redispatch, calculated assuming steady-state conditions, is executed with G211 and G206.

Shifting the power injection changes the load flows and losses. They are balanced in the steady-state calculation by the slack. By contrast, a positive frequency deviation results in dynamic simulation because of the different rates of change of generators (Figure 4, section 2), which is partially balanced by the primary control. The power injected by 101G1 (Figure 4, black) is increased in order to correct this frequency deviation. The line power flow is reduced to 1016 MW by generator redispatch. The result is heavily affected by the generators, which are part of the primary control. Since the location of generators in area 1 (see Fig. 1), requiring a reduction in the power supplied, affects the line power flow adversely, the active power flow is only reduced to 1016 MW instead of 1000 MW. The primary control is replaced by the secondary control (Fig. 4). If this is performed at the generator G206, which is stepped up another 80 MW after 200 s in order to compensate for the frequency deviation, it will reduce the active power flow to the 1000 MW required. The location of the generator providing secondary control also affects the results.

The effect of the fault and the measure on the active power flow through the line and on the LPFI of line 13 is presented in Figure 5. After the fault, the LPFI increases up to 0.9, a critical overload. The line is still heavily loaded after the measure, but not critically since the value is below 0.75.

Similar results for redispatch by the load-generator combination are presented in Fig. 6 and 7. The power flow can also be reduced as required with this combination.

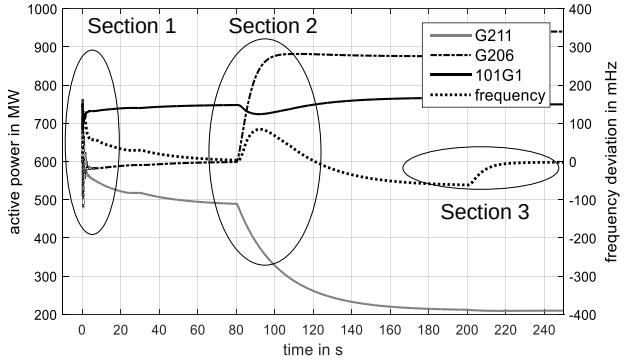

Figure 4. Redispatch by generator couple, change in active power injection.

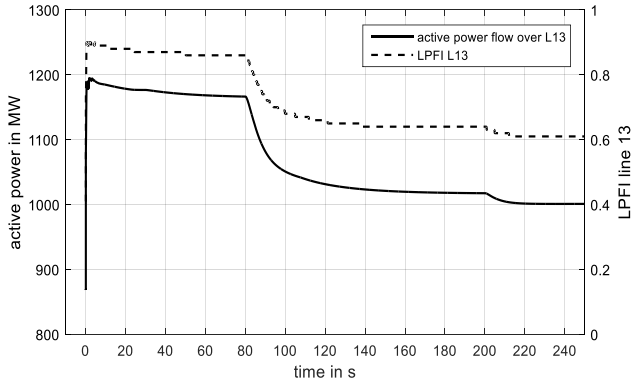

Figure 5. Redispatch with generators, dependence of the LPFI and the active power flow through the line.

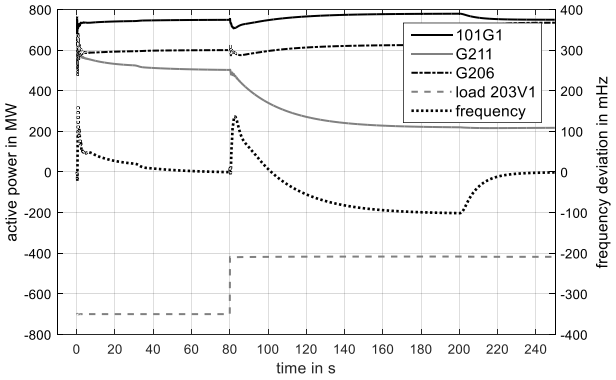

Figure 6. Redispatch by load-generator combination, change in active power injection.

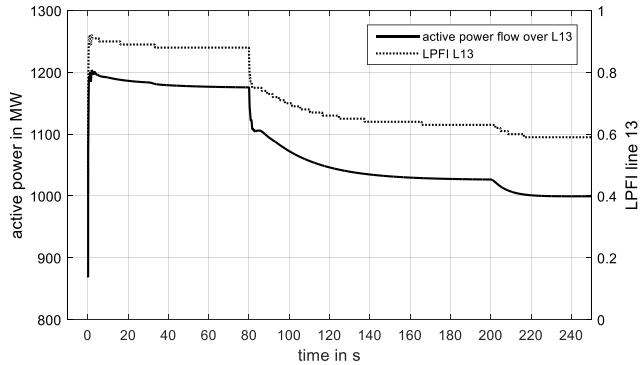

Figure 7. Redispatch with load generator combination, the dependence of the LPFI and the active power flow through the line.

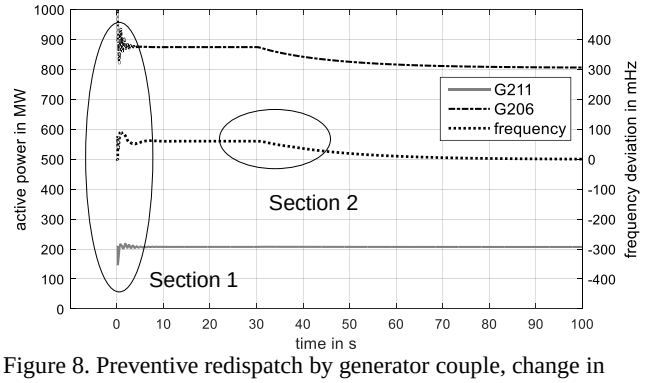

Figure 8. Preventive redispatch by generator couple, change in active power injection.

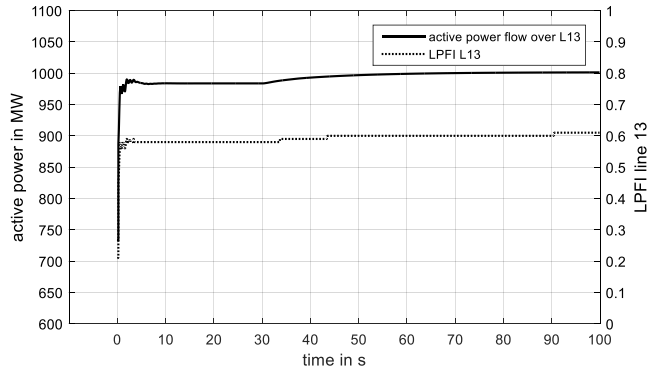

Figure 9. Preventive redispatch with generators, the dependence of the LPFI and the active power flow over the line.

Redispatch measures are usually performed preventively. For test purposes, the preventive measure is calculated based on the system initial state and the changed test system topology (switched off line 14). For this reason, the generator speed control that is active after the disturbance is disregarded. This results in a significantly larger redispatch of ΔPr = 392 MW. The results of changing generator power injection before the contingency are presented in Figure 8 and Fig. 9. The preventive measure prevents the LPFI from reaching the critical value of 0.75.

3) Discussion

The comparison of the total adjustment required in remedial P_{CUR} and preventive redispatch P_{PRE} including the reserve yields the following:

- $P_{\mathrm{PRE}} = \Delta P_{\mathrm{r}} + P_{\mathrm{RES}} = 971$ MW
- $P_{\mathrm{CUR}} = \Delta P_{\mathrm{r}} + P_{\mathrm{RES}} = 615$ MW

Since a preventive redispatch measure obviously requires more active power adjustment than a remedial redispatch measure, redispatch measures can be optimized when the generators' dynamic performance is factored in.

The suitability of steady-state methods for calculating optimal redispatch based on information from a dynamic security assessment system has also been demonstrated.

All of the results from the SIGURAD DSA tool are demonstrated in Fig. 10. The transient stability indices implemented are displayed on the left and the resultant

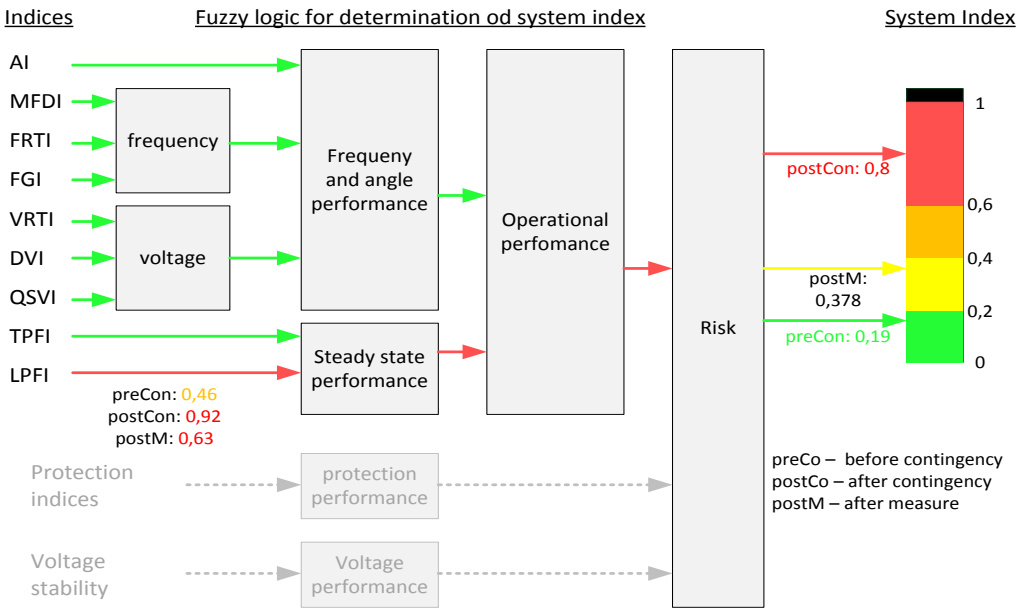

Figure 10. Results from SIGUARD®DSA tools.

system index summarizing system risk is displayed on the right. Readers are referred to [49], [6] for details of the index description. The SIGURAD®DSA also includes a voltage stability assessment as well as a wide area protection scheme based on [55] to incorporate adaptive protection schemes in the future [56].

Fig. 10 presents three different system states:

1. the system state before a contingency
2. the system state after the contingency, and
3. the system state after implementation of the proposed measure.

All indices in system state 1 are green, except LPFI, which is orange (0.46). The fuzzy logic aggregates standalone indices into a system index, which is green (lower system risk) for state 1. Line 14 is switched off in state 2. The resultant congestion problem is also evident in the system index, which rises from 0.19 to 0.8 after this contingency. This is a consequence of the higher LPFI of line 13, which increased from 0.46 to 0.92. Once the measure is implemented, the system index decreases to 0.378. Other indices are not affected.

V. Conclusion

The extension of the Newton-Raphson (NR) algorithm for optimal generator adjustment [34] has been adapted in this study to factor in the slack generator and loads for redispatch, and the effectiveness of the new algorithm with these extensions has been demonstrated. Since a comparison with a method based on PTDF yields good agreement, the proposed algorithm can be applied.

The load-generator combinations and load combinations constitute the most efficient method with the lowest power adjustment for a smart grid with controllable loads.

Furthermore, the ENRA-RM method, which determines redispatch based on a steady-state operating point, has been shown to produce excellent results in dynamic simulation. Deviations caused by the steady-state analysis are compensated by an intelligent choice of secondary control. This makes it suitable for calculating countermeasures in a system's security assessment system. Moreover, preventive redispatch measures were shown to require more active power adjustment than remedial redispatch measures. Redispatch measures can therefore be optimized when the system's dynamic performance is factored in and DSA is employed.

The ENRA method can also be adapted for voltage problems. Since voltage problems can be protracted problems, the feasibility of applying this method to adjust components during voltage problems will have to be tested in future studies.

VI. References

[1] 50Hertz Transmission GmbH, „Veröffentlichungspflichtige EEG Daten," [Online]. Available: http://www.50hertz.com/de/EEG (in German)

[2] P. Kundur, J. Paserba, V. Ajjarapu, G. Andersson, A. Bose, C. Canizares, N. Hatziargyriou, D. Hill, A. Stankovic, C. Taylor, T. Van Cutsem and V. Vittal, „Definition and Classification of Power System Stability, IEEE/CIGRE Joint Task Force on Stability Terms and Definitions," *IEEE Transaction on Power Systems*, vol. 19, no. 2, 2004.

[3] T. van Cutsem and C. Vournas, Voltage Stability of Electric Power Systems, Springer Science & Business Media, 2007.

[4] P. Kundur, N. J. Balu and M. G. Lauby, Power System Stability and Control, McGraw-Hill

Education, 1994.

[5] A. Bihain, D. Cirio, M. Fiorina, R. Lopez, C. Lucarella, S. Massucco, D. Ruiz Vega, C. Vournas, T. Van Cutsem and L. Wehenkel, „OMASES: A DYNAMIC SECURITY ASSESSMENT TOOL FOR THE NEW MARKET ENVIRONMENT," in *IEEE Bologna Power Tech Conference*, Bologna, Italy, 2003.

[6] C. O. Heyde, R. Krebs, O. Ruhle and Z. A. Styczynski, „Dynamic voltage stability assessment using parallel computing," in *IEEE Power and Energy Society General Meeting*, Minneapolis, 2010.

[7] I. Chychykina, Z. A. Styczynski, C. O. Heyde and R. Krebs, „Power System instability prevention and remedial measures with online Dynamic Security Assessment," in *IEEE PowerTech*, Eindhoven, 2015.

[8] I. Hauer, M. Wolter, M. Stötzer, M. Richter and Z. A. Styczynski, „A probabilistic load shedding concept considering highly volatile local generation," *International Journal of Electrical Power and Energy Systems*, 67, pp. 478-487, 2015.

[9] T. Van Cutsem and C. D. Vournas, „Emergency voltage stability controls: An overview," in *IEEE/PES General Meeting*, Tampa, USA, 2007.

[10] D. Wang, S. Parkinson, W. Miao, H. Jia, C. Crawford and N. Djilali, „Online voltage security assessment considering comfort-constrained demand response control of distributed heat pump systems" *Applied Energy*, vol. 96, pp. 104-114, 2012.

[11] C. D. Vournas, C. Lambrou and M. Kanatas, „Application of Local Autonomous Protection Against Voltage Instability to IEEE Test System," *IEEE TRANSACTIONS ON POWER SYSTEMS*, vol. 31, no. 4, July 2016.

[12] A. Pillay, S. Prabkakar Karthikeyan and D. P. Kothari, „Congestion management in power systems – A review," *International Journal of Electrical Power & Energy Systems*, no. 70, pp. 83-90, 2015.

[13] S. S. Song, C. H. Park, M. Yoon und G. Jang, „Implementation of PTDFs and LODFs for Power System Security," *Journal of International Council on Electrical Power Engineering*, vol. 1, no. 1, pp. 49-53, 2011.

[14] M. Esmaili, H. A. Sayanfer and N. Amjady, „Congestion management enhancing transient stability of power system," *Applied Energy, 87 (3)*, pp. 971-981, 2010.

[15] D. Sosic and I. Skokljev, „Evolutionary algorithm for calculating available transfer capability," *Journal of Electrical Engineering*, vol. 64, no. 5, pp. 291-297, 2013.

[16] M. Patel and A. A. Girgis, „Review of available transmission capability (ATC) calculation methods," in *Power Systems Conference*, Clemson, 2009.

[17] N. D. Ghawghawe and K. L. Thakre, „Application of power flow sensitivity analysis and PTDF for determination of ATC," in *IEEE conference on Power Electronics Drives and Energy Systems*, 2006.

[18] H. Saadat, Power System Analysis, McGraw Hill Higher Education, 2002.

[19] S. A. Hosseini, N. Amjady, M. Shafie-khah and J. P. S. Catalao, „A new multi-objective solution approach to solve transmission congestion management problem of energy markets," *Applied Energy*, vol. 165, pp. 462-471, 2016.

[20] M. Esmaili, F. Ebadi, H. A. Shayanfar and S. Jadid, „Congestion management in hybrid power markets using modified Benders decomposition," *Applied Energy*, vol. 102, pp. 1004-1012, 2013.

[21] S. Gope, A. Kumar Goswami, P. Kumar Tiwari and S. Deb, „Rescheduling of real power for congestion management with integration of pumped storage hydro unit using firefly algorithm," *International Journal of Electrical Power & Energy Systems*, no. 83, pp. 434-442, 2016.

[22] X. Jia, „Transmission congestion management method based on coupon incentive mechanism," *Dianwang Jishu Power System Technology*, no. 37, pp. 1291-1297, 2013.

[23] P. Saino and D. Sarno, „Assessing the benefits of residential demend resposnse in a real time distribution energy market," *Applied Energy*, vol. 161, pp. 553-551, 2016.

[24] M. Stötzer, M. Richter, I. Hauer and Z. A. Styczynski, „Potential of demand-side integration to maximize the use of renewable energy sources in Germany," *Applied Energy*, vol. 146, pp. 344-352, 2015.

[25] B. K. Talukar, A. K. Sinha, S. Mukhopadhyay and A. Bose, „A computationally simple method for cost-efficient generation rescheduling and load shedding for congestion management," *Eleenergy systemsctrical power and energy systems*, vol. 27, pp. 379-388, 2005.

[26] L. Chen, H. Suzuki, T. Wachi and Y. Shimura, „Components of nodal prices for electric power systems," *IEEE Transaction on Power Systems*, 17(1), pp. 41-49, 2002.

[27] G. Yesuratnam and D. Thukaram, „Congestion managements in open access based on relative electrical distance using voltage stability criteria," *Electric Power System Reseach*, 77 (12), pp. 1608-1618, 2007.

[28] J. Hazra and A. Sinha, „J. Hazra, A.K. Sinha: Congestion management using multiobjective

particle swarm optimization," *IEEE Transaction on Power Systems*, 22(4), pp. 1726-1734., 2007.

[29] K. Van Den Bergh, D. Couckuyt, E. Delarue and E. D´Haeseleer, „Redispatching in an interconnected electricity system with high renewables penetration," *Electric Power Systems Research*, vol. 127, pp. 64-72, 10 June 2015.

[30] N. M. Bachtiar, A. Arief and R. C. Bansal, „Transmission management for congested power system: A review of concepts, technical challenges and development of a new methodology," *Renewable and Sustainable Energy Reviews*, vol. 38, pp. 572-580, October 2014.

[31] I. Bielchev, M. Richter, M. Banka, P. Trojan, Z. Styzsnski, Naumann, A and P. Komarnicki, „Dynamic distribution grid management through the coordination of decentralized power units," in *IEEE Power and Energy Society General Meeting*, Detroit, 2015.

[32] K. Singh, V. Yadav, N. Padhy and J. Sharma, „Congestion management considering optimal placement of distributed generator in deregulated power system networks," *Electric Poaer Components and Systems, 42(1),* pp. 13-22, 2014.

[33] B. Singh, R. Mahanty and S. Singh, „Optimal rescheduling of generators for congestion management and benefit maximization in a decentralized bilateral multi-transactios power network," *International Journal if Emerging Electric Poaer Systems, 14(1),* pp. 25-32, 2013.

[34] M. Glavic and F. Alvarado, „An extension of Newton–Raphson power flow problem," *Applied mathematics and computation,* vol. 186, pp. 1192-1204, 2007.

[35] B. R. O. Dietrich Oeding, Elektrische Kraftwerke and Netze, Springer-Verlag Berlin Heidelberg, 2011.

[36] M. Wolter, *Agent based energy management systems, Habilitation,* Shaker Verlag, 2012.

[37] T. Leveringhaus and L. Hofmann, „Comparison of methods for state prediction: Power Flow Decomposition (PFD), AC Power Transfer Distribution factors (AC-PTDFs), and Power Transfer Distribution factors (PTDFs)," in *Power and Energy Engineering Conference (APPEEC), 2014 IEEE PES Asia-Pacific, DOI: 10.1109/APPEEC.2014.7066183*, 7.-10.12.2014.

[38] O. Alsac and B. Stott, „Optimal Load Flow with Steady-State Security," *IEEE Transactions on Power Apparatus and Systems*, vol. 93, no. 3, pp. 745-751, 1974.

[39] R. D. Zimmerman, C. E. Murillo-Sanchez and R. J. Thomas, „MATPOWER: Steady-State Operations, Planning, and Analysis Tools for Power Systems Research and Education," *IEEE Transactions on Power Systems*, vol. 26, no. 1, pp. 12-19, 2011.

[40] J. Sun and K. L. Lo, „A congestion management method with demand elasticity and PTDF approach," in *47th International Universities Power Engineering Conference (UPEC)*, 2012.

[41] C. Klabunde, N. Moskalenko, P. Lombardi, Z. A. Styczynski and P. Komarnicki, „Optimal onshore wind power integration supported by local Energy Storages," in *IEEE Power and Energy Society General Meeting*, Detroit, 2015.

[42] C. Klabunde, N. Moskalenko, Z. A. Styzynski, P. Lombardi and P. Komarnicki, „Use of energy storage systems in low voltage networks with high photovoltaic system penetration," in *IEEE PowerTech*, Eindhoven, 2015.

[43] T. Sokolnikova, K. Suslov, P. Lombardi, I. Hauer and Z. A. Styczynski, „Use of economic index for optimal storage dimensioning within an autonomous power system," in *IEEE PowerTech*, Grenoble, France, 2013.

[44] J. Heuer, P. Komarnicki and Z. A. Styczsnki, „Integration of elecrical vehicles into the Smart grid in the Harz.EE-mobility research project," in *IEEE Power and Energy Society General Meeting*, Detroit, 2011.

[45] A. Naumann, I. Bielchev, N. Voropai and Z. A. Styczynski, „Smart Grid automation using IEC 61850 and CIM Standards," *Control Engineering Practice*, 25(1), pp. 102-111, 2014.

[46] C. O. Heyde, Dynamic Voltage Security Assessment for On-Line Control Room Application, Magdeburg, Dissertation, 2010.

[47] C. O. Heyde, R. Krebs and Z. A. Styczynski, „Optimal bottleneck prevention in transmission systems using dynamic security assessment," in *IEEE Power and Energy Society General Meeting*, San Diego, 2012.

[48] C. O. Heyde, R. Krebs and Z. A. Styczynski, „Short-Term Forecasts incorporated in Dynamic Security Assessment of Power Systems," IEEE Generalmeeting, Detroit, 2011.

[49] U. Kerin, *Development of tools for dynamic security assessment of electric power systems, Dissertation,* Ljubljana, 2010.

[50] U. Kerin and E. Lerch, „Dynamic Security Assessment to Improve System Stability," in *IEEE EPU-CRIS International Conference on Science and Technology*, Hanoi, Vietnam , 2011.

[51] J. Martchamadol and S. Kumar, „An aggregated energy security performance indicator," *Applied Energy*, vol. 103, pp. 653-670, 2013.

[52] H. Nguyen-Duc, I. Kamwa, L. A. Dessaint and H. Cao-Duc, „A Novel Approach for Early Detection of Impending Voltage Collapse Events Based on the Support Vector Machine," *International Transactions on Electrical Energy Systems*, 2017.

[53] C. Liu , K. Sun, Z. H. Rather , Z. Chen , L. C. Bak, P. Thøgersen and P. Lund, „A Systematic Approach for Dynamic Security Assessment and the Corresponding Preventive Control Scheme Based on Decision Trees,“ *IEEE Transactions on Power Systems*, Oktober 2013.

[54] C. Liu, C. L. Bak and Z. Chen, „Dynamic security assessment of western Danish power system based on ensemble decision trees,“ in *12th IET International Conference on Developments in Power System Protection*, Copenhagen, Denmark , 2014.

[55] M. Dauer, J. Jäger, T. Bopp and R. Krebs, „ Protection Security Assessment - System Evaluation Based on Fuzzification of Protection Settings,“ in *IEEE ISGT Europe*, Kopenhagen, 2013.

[56] A. G. Phadke, P. Wall, L. Ding and V. Terzija, "Improving the performance of power system protection using wide area monitoring systems," *Journal of Modern Power Systems and Clean Energy*,vol. 4, No. 3, pp. 319-331, 2016.

Ines Hauer studied mechatronics at the Otto-von-Guericke-University Magdeburg and received a diploma degree in 2010. Since 2010 she has worked as a scientific assistant at the Chair of Electric Power Networks and Renewable Energy Sources at Otto-von-Guericke-University, Germany. She received the Ph.D degree in 2014. Since 2017 she has been assistant professor for energy storage systems at the Otto-von-Guericke-University Magdeburg. Her research interests include power system stability, renewables integration, and energy storage systems.

Marc Richter worked as a graduate assistant in the Department of Electric Power Systems of Otto von Guericke University Magdeburg in Germany from 2012 to 2017. He was awarded his doctorate, summa cum laude, for his dissertation on the observability of electrical grids in 2016. At present, he is a research scientist in the Convergent Infrastructures Business Unit of the Fraunhofer Institute for Factory Operation and Automation IFF. His research interests include power system monitoring, renewables integration, and the application of industrial demand response to problems in convergent infrastructures.

Chris Oliver Heyde graduated in 2005 from Otto-von-Guericke University in Magdeburg, Germany, with the Dipl.-Ing. degree in electrical engineering. From 2005 to 2010 he worked as a scientific assistant at the Chair of Electric Power Networks and Renewable Energy Sources of the same university. He received the Ph.D degree in 2010. Since 2010 he has worked at Siemens Power Technology International as a consultant.